Vapor−Liquid Equilibrium, Coexistence Curve, and Critical Locus for Pentafluoroethane + 1,1,1,2-Tetrafluoroethane (R125/R134a)

Yukihiro Higashi[†]

Department of Mechanical Engineering, Iwaki Meisei University, 5-5-1, Iino, Chuodai, Iwaki 970-8551, Japan

The vapor−liquid equilibrium for pentafluoroethane (R125) + 1,1,1,2-tetrafluoroethane (R134a) was measured along four isotherms between 283 K and 313 K. The vapor−liquid coexistence curve at constant composition near the mixture critical point was measured by the observation of the meniscus disappearance. The critical temperatures and critical densities of the 0.2670 and 0.6648 mole fraction of R125 were determined from the saturation densities along the coexistence curve in the critical region. In addition, the critical locus for the R125/R134a mixture is correlated as a function of composition.

Introduction

Because of their low ozone-depletion potentials, hydrofluorocarbon (HFC) mixtures are considered as alternative refrigerants for chlorodifluoromethane (R22) and R502 (an azeotrope of R22 and R115) as the working fluids of air conditioning and heat pump systems. Ternary mixtures of difluoromethane (R32), pentafluoroethane (R125), and 1,1,1,2-tetrafluoroethane (R134a), especially the mixtures R407C (23 mass % R32 + 25 mass % R125 + 52 mass % R134a) and R407E (25 mass % R32 + 15 mass % R125 + 60 mass % R134a), are of interest as candidates for replacing R22. In addition, ternary mixtures of R125, R134a, and 1,1,1-trifluoroethane (R-143a), especially the mixture R404A (44 mass % R125 + 52 mass % R-143a + 4 mass % R134a), are of interest as candidates for replacing R502. However, reliable information on the thermophysical properties of these mixtures is insufficient.

The present author has previously measured the vapor−liquid equilibrium and the critical locus for the R32/R134a mixture (Higashi, 1995) and for the R32/R125 mixture (Higashi, 1997). This paper reports similar equilibrium measurements for the R125/R134a mixture.

Experimental Section

Chemicals. The samples of pure R125 and pure R134a were furnished by Asahi Glass Co. Ltd. (To describe materials and experimental procedures adequately, it is occasionally necessary to identify commercial products by the manufacturer's name or label. Such identification does not imply recommendation or endorsement by the National Institute of Standards and Technology nor does it imply that the particular material or equipment is necessarily the best available for the purpose). The stated sample purities were 99.99 mass % R125 and 99.99 mass % R134a. These samples were used without further purification.

Apparatus for Vapor−Liquid Equilibrium Measurements. The experimental apparatus for measuring the vapor−liquid equilibrium has been described in detail previously (Higashi, 1995, 1997). Temperatures were measured with a 100 Ω platinum resistance thermometer immersed in a thermostated bath. This thermometer was located in the vicinity of the equilibrium cell and calibrated against ITS-90 using a 25 Ω standard platinum resistance thermometer. The uncertainty of temperature measurements is estimated to be within ±10 mK. The pressure of the sample was measured with a diaphragm semiconductor strain-gauge pressure transducer. This pressure transducer was installed in the cell and can measure the fluid pressure directly. The pressure transducer calibration was checked against a quartz crystal pressure transducer after each series of experiments. The uncertainty of the pressure measurement is estimated to be within ±3 kPa. Compositions of the vapor phase (dew-point composition) and the liquid phase (bubble-point composition) for the mixtures were determined using a gas chromatograph equipped with a thermal conductivity detector. The mixtures for the calibration were prepared gravimetrically from components with the above-stated purity. The uncertainty of the composition measurement is estimated to be within ±0.4 mol %.

Apparatus for Vapor−Liquid Coexistence Curve Measurements. The measurements of the vapor−liquid coexistence curve near the critical point were based on the observation of the meniscus disappearance. The author has already described in detail the experimental apparatus (Higashi, 1994).

The main portion of the apparatus is composed of three pressure vessels, that is, an optical cell with two Pyrex windows, an expansion vessel used to change the sample density in the optical cell without a new sample charge, and a supply used to change the sample density and prepare the initial sample mixture. The apparatus was installed in a thermostated silicone oil bath. The bath temperature can be kept constant within ±5 mK. Temperature measurements are made with a 25 Ω standard platinum resistance thermometer calibrated against ITS-90 with the aid of a thermometer bridge. The thermometer was mounted in the vicinity of the optical cell. The uncertainty of temperature measurement is estimated to be within ±10 mK.

The sample density in the optical cell can be calculated from the mass of the sample and the inner volume of the three vessels. In the present measurement, the expansion procedure was introduced to change the sample density in the optical cell. It is unavoidable that the experimental uncertainty in the density measurements is directly proportional to the total number of expansions. The uncer-

---

[†] Present address: Guest Researcher at the Physical and Chemical Properties Division, Chemical Science and Technology Laboratory, National Institute of Standards and Technology, Boulder, Colorado 80303.

10.1021/je980265h CCC: $18.00

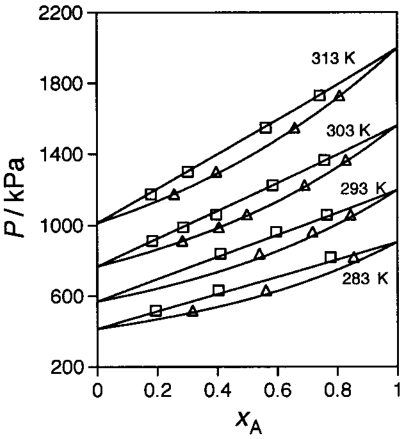

Figure 1. Vapor–liquid equilibria of the R125 (A)/R134a (B) mixture in the pressure–temperature diagram: (□) bubble-point; (△) dew-point; (–) REFPROP 6.0 predictions.

Table 1. Isothermal Vapor–Liquid Equilibrium Data of the R125(A)/R134a(B) Mixture

T/K	P/kPa	x_A	y_A
283.05	516.7	0.1937	0.3171
283.15	632.1	0.4039	0.5614
283.05	819.0	0.7761	0.8540
293.15	838.3	0.4100	0.5400
293.05	962.5	0.5958	0.7167
293.05	1059.4	0.7650	0.8435
303.04	912.9	0.1830	0.2835
303.15	990.1	0.2857	0.4049
303.04	1060.1	0.3962	0.4981
303.04	1226.4	0.5844	0.6909
303.04	1365.5	0.7563	0.8283
313.04	1175.9	0.1793	0.2561
313.15	1301.7	0.3022	0.3965
313.04	1548.0	0.5614	0.6582
313.04	1730.9	0.7413	0.8076

tainty of the density measurements is different for each measurement in this work. The number of expansions was restricted to maintain the uncertainty of density measurement within ±0.5%.

For the preparation of the sample mixture with a prescribed density and composition, additional pressure vessels were used. Each vessel was filled with the appropriate pure components and weighed on a precision balance (capacity of 3 kg and resolution of 0.05 mg) with an uncertainty of ±2 mg. Whenever any overestimation of the mass of components was found, the component fluid had to be discharged to the necessary extent. Then each component was transferred successively to the supply vessel evacuated to 0.5 mPa and cooled by liquid nitrogen. It was estimated that the uncertainty of the mass of the sample thus obtained was not greater than ±0.1%. In addition, the uncertainty of the composition of the sample was estimated to be within ±0.05%. In this experiment, a gas chromatograph is not used to determine the composition.

Experimental Results

Vapor–Liquid Equilibrium. The experimental results for the vapor–liquid equilibrium (VLE) for the R125/R134a mixture are given in Table 1. Measurements were made along four isotherms, i.e., (283, 293, 303, and 313) K. The distribution of VLE results for the R125/R134a mixture is shown in Figure 1 on a pressure–composition diagram. In this figure, the solid lines are the predictions of REFPROP 6.0 (McLinden et al., 1998) at the same four temperatures.

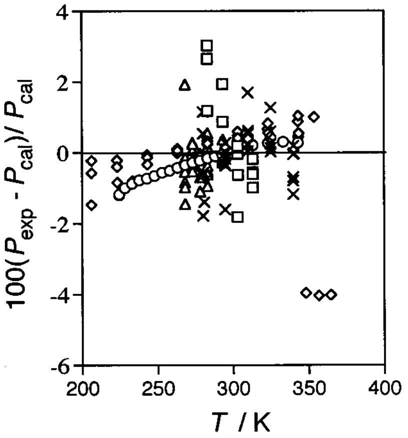

Figure 2. Bubble-point pressure deviations of the experimental VLE data from the predictions of REFPROP 6.0 for the R125 (A)/R134a (B) mixture vs temperature: (□) present work; (◇) Nagel and Bier (1995); (○) Kleemiss (1996); (×) Holcomb et al. (1997); (△) Kobayashi and Nishiumi (1998).

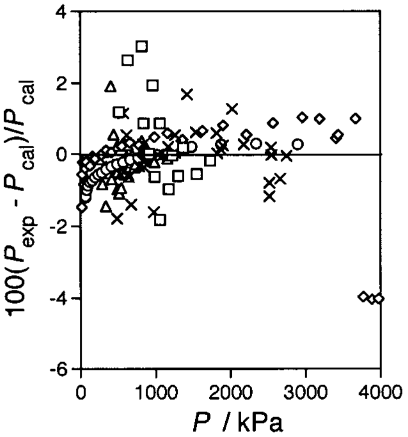

Figure 3. Bubble-point pressure deviations of the experimental VLE data from the predictions of REFPROP 6.0 for the R125 (A)/R134a (B) mixture vs pressure: (□) present work; (◇) Nagel and Bier (1995); (○) Kleemiss (1996); (×) Holcomb et al. (1997); (△) Kobayashi and Nishiumi (1998).

Experimental results for the vapor–liquid equilibrium for the R125/R134a mixture measured by Nagel and Bier (1995), Kleemiss (1996), Holcomb et al. (1997), and Kobayashi and Nishiumi (1998) were available for comparison. The bubble-point pressure comparisons between the available VLE data and the calculated results of REFPROP 6.0, using the Helmholtz free energy model equation of state (Lemmon and Jacobsen, 1997), are shown in Figures 2–4. These deviations are plotted against temperature, pressure, and composition in Figures 2–4, respectively. As shown in Figures 2–4, the bubble-point pressure deviations between the experimental VLE data including the present data, and the calculated results of the Helmholtz free energy model equation of state in REFPROP 6.0 are in good agreement within an uncertainty of ±2%, although two data points at the lowest temperature from this work show a larger deviation.

The dew-point composition comparisons between the available VLE data and the calculated results of the Helmholtz free energy model equation of state are shown in Figures 5–7. To calculate the dew-point compositions, the mixture parameters of the Helmholtz free energy model equation of state were adopted from REFPROP 6.0. The available VLE data agree with each other. In addition, the Helmholtz free energy model equation of state adopted in REFPROP 6.0 can reproduce most of the VLE data within a mole fraction deviation range from +0.01 to −0.02.

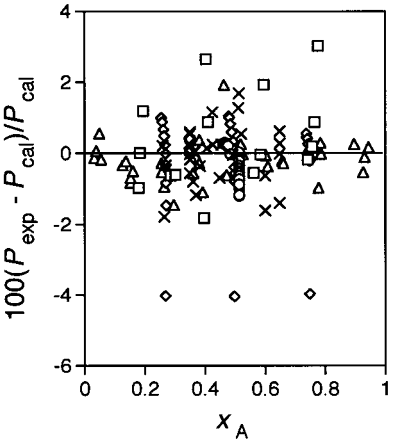

Figure 4. Bubble-point pressure deviations of the experimental VLE data from the predictions of REFPROP 6.0 for the R125 (A)/R134a (B) mixture vs bubble-point composition of R125: (□) present work; (◇) Nagel and Bier (1995); (○) Kleemiss (1996); (×) Holcomb et al. (1997); (△) Kobayashi and Nishiumi (1998).

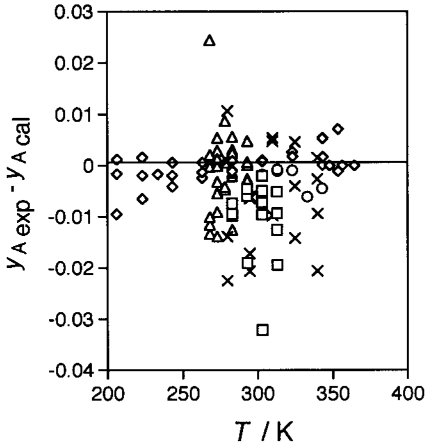

Figure 5. Dew-point composition deviations of the experimental VLE data from the predictions of REFPROP 6.0 for the R125 (A)/R134a (B) mixture vs temperature: (□) present work; (◇) Nagel and Bier (1995); (○) Kleemiss (1996); (×) Holcomb et al. (1997); (△) Kobayashi and Nishiumi (1998).

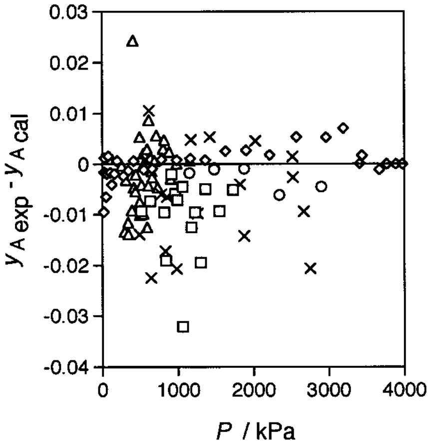

Figure 6. Dew-point composition deviations of the experimental VLE data from the predictions of REFPROP 6.0 for the R125 (A)/R134a (B) mixture vs pressure: (□) present work; (◇) Nagel and Bier (1995); (○) Kleemiss (1996); (×) Holcomb et al. (1997); (△) Kobayashi and Nishiumi (1998).

Vapor−Liquid Coexistence Curve near the Critical Point. The vapor−liquid coexistence curves near the critical point for the 26.70 mol % R125 + 73.30 mol %

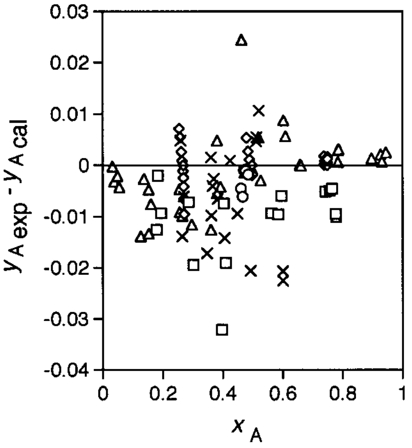

Figure 7. Dew-point composition deviations of the experimental VLE data from the predictions of REFPROP 6.0 for the R125 (A)/R134a (B) mixture vs bubble-point composition of R125: (□) present work; (◇) Nagel and Bier (1995); (○) Kleemiss (1996); (×) Holcomb et al. (1997); (△) Kobayashi and Nishiumi (1998).

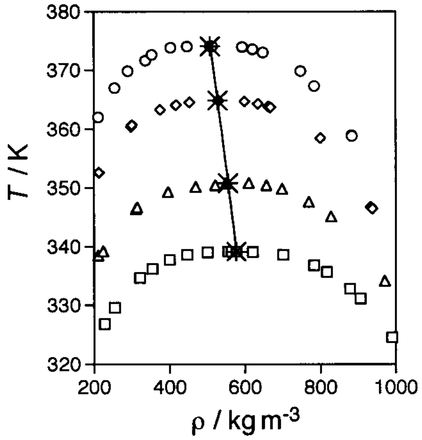

Figure 8. Vapor−liquid coexistence curves of the R125 (A)/R134a (B) mixture in the critical region: (*) critical point; (−) critical locus; (○) $x_A = 0.0$; (◇) $x_A = 0.2670$; (△) $x_A = 0.6648$; (□) $x_A = 1.0$.

Table 2. Vapor−Liquid Coexistence Curve Data for R125(A)/R134a(B) System near the Critical Point

$x_A = 0.2670$		$x_A = 0.6648$	
T/K	ρ/kg m^{-3}	T/K	ρ/kg m^{-3}
346.45	938.2 ± 0.9	334.18	970.2 ± 0.9
346.73	933.4 ± 0.9	345.15	828.0 ± 0.8
358.43	800.2 ± 0.8	347.64	769.3 ± 1.3
363.69	668.0 ± 0.7	349.82	698.4 ± 0.7
363.84	662.3 ± 0.7	350.44	656.8 ± 1.2
364.32	634.8 ± 1.1	350.80	610.4 ± 0.7
364.70	599.0 ± 0.6	350.81	554.2 ± 1.0
364.84	530.0 ± 0.9	350.74	549.2 ± 1.7
364.89	528.3 ± 1.7	350.44	521.2 ± 1.6
364.55	453.2 ± 1.4	350.14	469.0 ± 1.5
364.07	417.0 ± 1.3	349.31	395.7 ± 0.9
363.27	375.2 ± 1.2	346.70	314.0 ± 1.2
360.70	300.3 ± 1.3	346.40	311.2 ± 1.7
360.36	297.8 ± 1.2	339.23	224.3 ± 1.2
352.60	212.7 ± 1.1	338.48	210.9 ± 1.3

R134a mixture and the 66.48 mol % R125 + 33.52 mol % R134a mixture were determined by visual observation of the meniscus disappearance. The experimental data obtained are given in Table 2 and shown in Figure 8 on the temperature−density plane. The experimental results of pure components reported by the author (Higashi, 1994) are also shown in Figure 8. The asterisk denotes the critical point, determined by taking into consideration the menis-

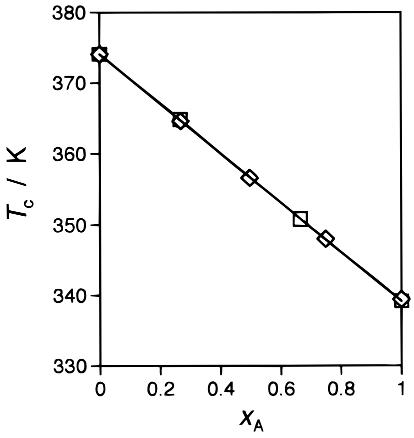

Figure 9. Composition dependence of the critical temperatures for the R125 (A)/R134a (B) mixture: (□) present author; (◇) Nagel and Bier (1995); (−) eq 1.

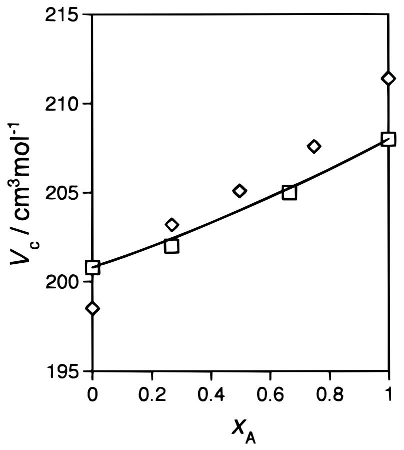

Figure 10. Composition dependence of the critical molar volumes for the R125 (A)/R134a (B) mixture: (□) present author; (◇) Nagel and Bier (1995); (−) eq 2.

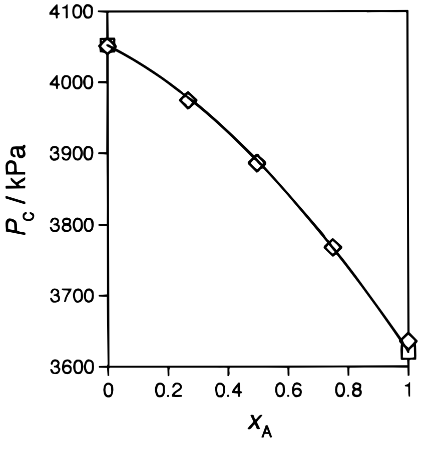

Figure 11. Composition dependence of the critical pressures for the R125 (A)/R134a (B) mixture: (□) present author; (◇) Nagel and Bier (1995); (−) eq 4.

cus disappearance level and the intensity of the critical opalescence. The solid line in Figure 8 shows the critical locus for the R125/R134a mixture. The critical temperature T_c, critical density ρ_c, and critical molar volume V_c of this mixture are summarized in Table 3. The critical locus on the temperature−density plane for the R125/R134a mixture is almost linear.

Table 3. Critical Parameters of the R125(A)/R134a(B) Mixture

x_A	T_c/K	ρ_c/kg m^{-3}	V_c/cm^3 mol^{-1}
0	374.11 ± 0.01	508 ± 5	201 ± 2
0.2670	364.84 ± 0.02	528 ± 3	202 ± 1
0.6648	350.81 ± 0.02	555 ± 3	205 ± 1
1	339.17 ± 0.01	577 ± 5	208 ± 2

Discussion

Correlation of the Critical Locus. To represent the composition dependence of the critical parameters for this system, a correlation of the critical locus was formulated. The functional forms of this correlation are as follows (Higashi et al., 1986; Higashi 1997):

$$T_{cm} = \theta_1 T_{c1} + \theta_2 T_{c2} + 2\theta_1\theta_2\Delta_T \tag{1}$$

$$V_{cm} = \theta_1 V_{c1} + \theta_2 V_{c2} + 2\theta_1\theta_2\Delta_V \tag{2}$$

$$\rho_{cm} = M_m/V_{cm} \tag*{(2)}$$

$$P_{cm} = \theta_1 P_{c1} + \theta_2 P_{c2} + 2\theta_1\theta_2\Delta_P \tag{4}$$

$$\theta_i = \frac{x_i V_{ci}^{\ 2/3}}{\sum_j x_j V_{cj}^{\ 2/3}} \tag{5}$$

Here T_{cm}, V_{cm}, ρ_{cm}, and P_{cm} denote the critical temperature of the mixture, the critical molar volume of the mixture, the critical density of the mixture, and the critical pressure of the mixture, respectively. M_m denotes the molar mass of the mixture and is $M_m = x_1M_1 + (1 - x_1)M_2$. The surface fraction θ_i is defined in eq 5 in terms of the composition and critical molar volumes of the pure components. Δ_T in eq 1, Δ_V in eq 2, and Δ_P in eq 4 are the adjustable parameters used to fit eqs 1, 2, and 4 to the data. The Δ_T and Δ_V values were determined from the present measured critical parameters of the two mixtures listed in Table 3. The Δ_P value was determined by taking into consideration the critical pressure of the R125/R134a mixture by Nagel and Bier (1995). With respect to the R125/R134a mixture, Δ_T, Δ_V and Δ_P are 0.4 K, −0.85 cm^3 mol^{-1}, and 0.11 MPa, respectively. By use of these adjustable parameters, the critical temperature of the mixture determined in the present study can be calculated within ±0.06 K. For the critical density of the mixture, the present correlation can represent our experimental results within the experimental uncertainty.

The comparisons of the critical temperature, critical molar volume, and critical pressure for the R125/R134a mixture between the present results and the Nagel and Bier's results are shown in Figures 9−11. For the critical temperature, the present results and Nagel and Bier's results are in good agreement. For the critical molar volume, both results did not agree not only as a mixture but also as a pure component.

Acknowledgment

The author is indebted to Messrs. M. Higuchi, T. Ikeda, and K. Kanai, Iwaki Meisei University, for their valuable assistance in this experiment. The author also thanks the Physical and Chemical Properties Division, National Institute of Standards and Technology for the opportunity to work as a Guest Researcher at NIST.

Literature Cited

Higashi, Y. Critical Parameters for HFC134a, HFC32 and HFC125. *Int. J. Refrig.* **1994**, *17*, 524−531.

Higashi, Y. Vapor-Liquid Equilibrium, Coexistence Curve and Critical Locus for Binary HFC-32/HFC-134a Mixture. *Int. J. Thermophys.* **1995**, *16*, 1175−1184.

Higashi, Y. Vapor-Liquid Equilibrium, Coexistence Curve, and Critical Locus for Difluoromethane + Pentafluoroethane (R-32 + R-125). *J. Chem. Eng. Data* **1997**, *42*, 1269−1273.

Higashi, Y.; Uematsu, M.; Watanabe, K. Measurements of the Vapor-Liquid Coexistence Curve and the Critical Locus for Several Refrigerant Mixtures. *Int. J. Thermophys.* **1986**, *7*, 29−40.

Holcomb, C. D.; Magee, J. W.; Scott, J. L.; Outcalt, S. L.; Haynes, W. M.; *Selected Thermodynamic Properties for Mixtures of R-32 (Difluoromethane), R-125 (Pentafluoroethane), R-134a (1,1,1,2-Tetrafluoroethane), R-143a (1,1,1-Trifluoroethane), R-41 (Fluoromethane), R-290 (Propane), and R-744 (Carbon Dioxide)*; NIST Technical Note 1397; NIST: Gaithersburg, MD, 1997.

Kleemiss, M. University of Hannover, private communication, 1996.

Kobayashi, M.; Nishiumi, H.; Vapor-Liquid Equilibria for the Pure, Binary and Ternary Systems Containing HFC32, HFC125 and HFC134a. *Fluid Phase Equilib.* **1998**, *144*, 191−202.

Lemmon, E. W.; Jacobsen, R. T. A Generalized Model for the Thermodynamic Properties of Mixtures. *Int. J. Thermophys.*, in press.

McLinden, M. O.; Klein, S. A.; Lemmon, E. W.; Peskin, A. P. REFPROP, Thermodynamic and Transport Properties of Refrigerants and Refrigerant Mixtures. *NIST Standard Reference Database 23*, version 6.0; NIST: Gaithersburg, MD, 1998.

Nagel, M.; Bier, K. Vapour-Liquid Equilibrium of Ternary Mixtures of the Refrigerants R32, R125 and R134a. *Int. J. Refrig.* **1995**, *18*, 534−543.

Received for review October 27, 1998. Accepted December 24, 1998.

JE980265H